Analysis of CrIS FM1 TVAC Test Data in Preparation for On-orbit Radiometric Calibration

Chunming Wang, Giovanni De Amici, Scott Farrow, Denise Hagan, Denis Tremblay
Northrop Grumman Aerospace Systems (NGAS)

1. Introduction

The Cross-track Infrared Sensor (CrIS) [1] is one of the key instruments for the National Polar-Orbiting Environmental Satellite System (NPOESS) [2]. As a Michelson interferometer, CrIS measures atmospheric emission spectrum in the infrared, which is to be used to produce the vertical temperature and moisture profiles of the Earth's atmosphere. The first Flight Module (FM1) of CrIS is to be launched on the NPOESS Preparatory Project (NPP) [3] satellite in 2011. As a part of prelaunch testing and characterization, the CrIS FM1 has undergone several phases of Thermal Vacuum tests; the last phase (TVAC3) of radiometric performance tests ended in December 2008. This paper presents the independent analyses of the TVAC3 test data of CrIS FM1 sensor by the NGAS team for NPP data product Calibration and Validation (Cal/Val). In addition to providing further verification of the instrument performance reported by the sensor manufacturer – ITT, our effort constitutes an important part of our preparation for the on-orbit Cal/Val of the CrIS FM1 data products. In particular, the residual radiometric calibration uncertainties, due in part to the limitations of TVAC test environment, led to our plan for on-orbit monitoring and further calibration. Sources of radiometric calibration uncertainties include: imperfect characterization of Internal Calibration Target (ICT) effective emissivity, detector nonlinearity, and the possible non-uniformity of the ICT surface brightness temperature. Our analyses of the TVAC data examine the sensitivity of the radiometric performance of CrIS FM1 to these parameters. In the remainder of this paper, we shall present the basic background information on the CrIS FM1 and its TVAC tests in Section 2. In Sections 3 and 4 we shall discuss the accuracy of the ICT radiance modeling and the accuracy of the detector nonlinearity correction, and the on-orbit monitoring of these issues. Our concluding remarks are in Section 5.

2. Background

The CrIS FM1 has 3 spectral bands -- Long-Wavelength IR (LWIR), Mid-Wavelength IR (MWIR) and Short-Wavelength IR (SWIR). Their characteristics are listed in Table 1 below.

Table 1. Spectral characteristic of CrIS FM1

	LWIR	MWIR	SWIR
Min Wave-number	650	1210	2155
Max Wave-number	1095	1750	2550
IGM Length	20,736	10,560	5,200
Decimation Factor	24	20	26
Number of Channels	864	528	200
SDR Channels	713	433	159

For each spectral band, a Focal Plane-Array (FPA) contains a rectangular 3 by 3 array of detectors, which provide the 9 Fields of View (FOV) of the instrument. During the normal operation of CrIS FM1, the Scene Selection Mirror (SSM) scans every 8 seconds in the direction perpendicular to the satellite velocity over 34 Fields of Regard (FOR) measuring an Interferogram (IGM) at each FOR. Among the 34 FORs, two IGMs are collected at the ICT and the Deep Space (DS) positions, respectively. The remaining 30 FORs are Earth Scene (ES) FORs. However, during the TVAC test, the instrument can also be commanded to stare at a particular FOR. The normal operational IGM is generated by the on-board digital processor from the full IGM after applying a complex pass-band filter and coarse sampling (or decimation). The instrument can also be commanded to deliver the full IGM by bypassing the filtering and decimation. These IGMs are referred to as Diagnostic IGMs.

During the TVAC tests the CrIS FM1 is placed in a chamber with two high emissivity blackbody calibration targets, the Space Target

(ST) and the External Calibration Target (ECT). During TVAC testing, the instrument's DS position is aligned with the ST. The ST is kept at a constant temperature of 107K, while the ECT temperature is set to various desired values ranging from 200K to over 310K. In order to evaluate the instrument's performance under different thermal environments, the temperature of the entire CrIS FM1 passes through 5 different plateaus, Proto-Qualifying Low (PQL), Mission Low (ML), Mission Nominal (MN), Mission High (HM) and Proto-Qualifying High (PQH), over the course of the TVAC test. Radiometric performance data are collected primarily over the PQL, MN and PQH plateaus.

The primary purpose of radiometric performance TVAC test of CrIS FM1 is to establish the accuracy of the calibrated radiance produced by the Sensor Data Record (SDR) generation algorithm, by comparing the values of the SDR to the expected ECT radiances at specified temperatures for each of nearly 1,400 spectral channels of each FOV. The basic calibration equation for each channel is given by

$$(1)\quad R_{ES}^{\lambda} = R_{DS}^{\lambda} + (R_{ICT}^{\lambda} - R_{DS}^{\lambda})\frac{I_{ES}^{\lambda} - I_{DS}^{\lambda}}{I_{ICT}^{\lambda} - I_{DS}^{\lambda}},$$

where R_{DS}^{λ} , R_{ICT}^{λ} correspond to estimated DS and ICT radiances, and R_{ES}^{λ} corresponds to the calibrated ES radiance; I_{DS}^{λ}, I_{ICT}^{λ} and I_{ES}^{λ} correspond to the raw spectra for the DS, ICT and ES, respectively. These raw spectra are obtained by performing a discrete Fourier transform of the IGMs for these FORs. Key factors contributing to the radiometric performance include the accuracy of the estimated ICT radiance and the linearity of the detectors that measure the IGMs. These issues are discussed in the following sections.

3. ICT Emissivity and Radiance Modeling

As shown in (1), the calibrated ES radiance depends on an accurate estimate of the radiance at the ICT position. This radiance, R_{ICT}^{λ} , is calculated using the measured temperature of the ICT and a model of its radiometric environment. The model is of the form

$$(2)\quad R_{ICT}^{\lambda} = \varepsilon_{ICT,eff}^{\lambda} BB(\lambda, T_{ICT}) + \left(1 - \varepsilon_{ICT,eff}^{\lambda}\right)\sum_{k=1}^{n} v_k \varepsilon_k BB(\lambda, T_k)$$

where $\varepsilon_{ICT,eff}^{\lambda}$ and ε_k^{λ} represent the effective surface emissivity of the ICT and the emissivity of *k*-th environmental component reflected by the ICT surface, respectively; $BB(\lambda, T)$ is the blackbody radiance given by the Planck function; T_{ICT} and T_k are the measured temperatures of the ICT and the *k*-th environmental components, and v_k is the fraction of the ICT surface that is reflecting the *k*-th component. The ICT radiometric environmental components include the SSM baffle, housing, ICT baffle and the space view. It is easy to see that the effective ICT emissivity plays a central role in this model. Ideally, we would like to have this emissivity be close to 1. In fact, a low value of $\varepsilon_{ICT,eff}^{\lambda}$ leads to an ICT radiance model that is sensitive to temperature measurement errors in the environmental components. A highly reliable independent and direct measurement of $\varepsilon_{ICT,eff}^{\lambda}$ is not available. Instead, the value of $\varepsilon_{ICT,eff}^{\lambda}$ is estimated during the TVAC test by interchanging the roles of R_{ES}^{λ} and R_{ICT}^{λ} in (1). Thus the radiance of ICT can be obtained by using as a calibration reference the expected ECT radiance given by the Planck function. Then the calibrated R_{ICT}^{λ} is used in (2) to derive a value for $\varepsilon_{ICT,eff}^{\lambda}$. It is not difficult to see from (2) that this approach can only lead to a stable result if substantial temperature differences exist between the temperatures of the ICT and its surrounding environmental components. To achieve a stable retrieval of $\varepsilon_{ICT,eff}^{\lambda}$, the TVAC test team intentionally lowered the temperature of the SSM baffle during the PQH plateau, thus creating a sufficient temperature difference between the SSM baffle and the ICT. The resulting retrieval of the $\varepsilon_{ICT,eff}^{\lambda}$ is shown in Figure 1.

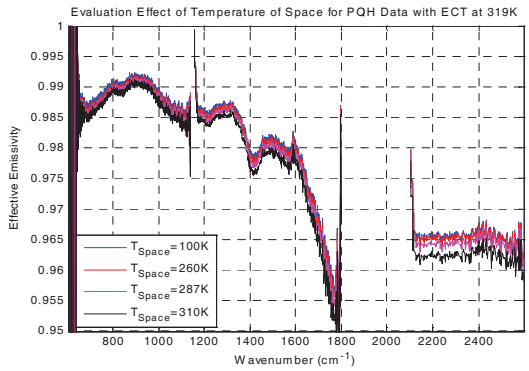

Figure 1. Retrieved value of $\varepsilon^{\lambda}_{ICT,eff}$ using TVAC3 PQH data with different temperatures for space view

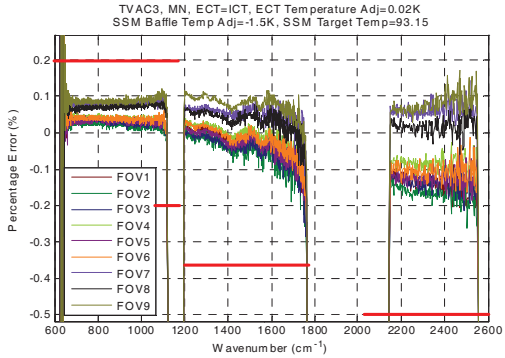

Figure 2. Excellent agreement is obtained between the calibrate ICT radiance for MN data and that predicted by the model based on the retrieved effective emissivity

The results in Figure 1 are obtained by averaging the calibrated ICT radiances for the 9 FOVs. In ITT's analysis, the entire effective emissivity curve is slightly adjusted upward, using the results of an independent measurement. By using the values provided by ITT, we have computed the ratio of the predicted ICT radiances to the calibrated ICT radiances, using the ECT as a calibration reference for data collected during the MN. The result is shown in Figure 2. In this comparison, we have adjusted the temperature of the ECT by 20mK, to remove an obvious temperature bias. In addition we have included a model-predicted SSM baffle temperature bias. The resulting radiance differences are well within the specification for the ICT radiance prediction accuracy, which is indicated by the red horizontal lines.

We also note that there are residual differences between FOVs. Within the limitations of the TVAC test, we are currently unable to conclusively determine whether or not these differences are caused by temperature variations across the ICT. These differences in the emissivity ascribed to the ICT can lead to differences in the range and the mean value of the calibrated ES radiances during on-orbit operation. Therefore, we identify the monitoring of differences in the mean and range of the ES radiances among different FOV as a key task during the on-orbit Cal/Val.

4. Detector Nonlinearity Characterization and Correction

The photovoltaic materials of a detector produce an electrical voltage when exposed to radiation. The nonlinear relationship between the incoming radiance and the voltage produced by a detector must be carefully characterized, and must then be corrected by the SDR processing algorithm. Assuming that a quadratic relationship is sufficient to accurately characterize the relationship between incoming radiance and the detector output voltage, a model of the measured IGM fringe intensity is given by

$$J_k = G\left((R_k + \bar{R}) + a_2(R_k + \bar{R})^2\right) - V_0, \quad (3)$$

where J_k and R_k are, respectively, the k-th measured IGM fringe heights and the incoming radiance to the detector array; G, $\bar{R}$ and V_0 are the gain and DC components of the incoming radiance and the detector, respectively, such that the resulting IGM has zero DC component, and a_2 is the quadratic coefficient of the nonlinear relationship. The frequency domain representation of this equation leads to

$$I_k = G\left((1 + 2a_2\bar{R})S_k + a_2(S \otimes S)_k\right), \quad (4)$$

where $\{S_k\}$ is the discrete Fourier transform of the sequence $\{R_k\}$. Two approaches to characterize the detector nonlinearity can be derived from (4). We note that in the frequency range of a spectral band, only the term $G(1 + 2a_2\bar{R})S_k$ is present. This leads to the nonlinearity correction algorithm for the SDR code [4], which consists of scaling the

raw spectrum I_k with a scene-dependent scalar $1+2a_2\bar{R}$ prior to the application of the calibration equation (1). At the same time, the value of a_2 can be determined empirically by adjusting the coefficient to minimize the residual nonlinearity in the calibrated radiance. The second approach uses the fact that in the low wave-number area of the spectrum, the term $S \otimes S$ dominates the spectrum. As a result, we can estimate a_2 if we know the value of G by using the equation

$$\frac{a_2}{G} \approx \frac{I_k}{(I \otimes I)_k}, \quad (5)$$

where k corresponds to a low wave-number spectral bin. This estimation approach requires the use of the diagnostic IGMs [5]. The values of a_2 obtained by the two approaches disagree somewhat, as seen in Figure 3.

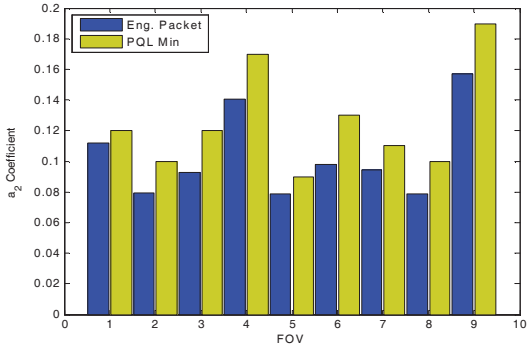

Figure 3. Comparison between a_2 coefficients retrieved by two different approaches

It is not surprising that the empirically derived a_2 coefficients in general yield better radiometric calibration performance than the values derived from (5).. The source of the difference in the values of a_2 is still not well-understood. Our analyses also indicate that the approach of retrieving a_2 using (5) leads to very stable results at different instrument plateaus and ECT temperatures, when only the DS or ICT IGM are used, as shown in Figure 4. The empirical approach of determining a_2 coefficient will obviously not be available during the on-orbit Cal/Val. We therefore must continue to investigate the possible reasons for the difference in the retrieved values. On the other hand, on-orbit monitoring and Cal/Val may allow us to better fine-tune the parameters for SDR code.

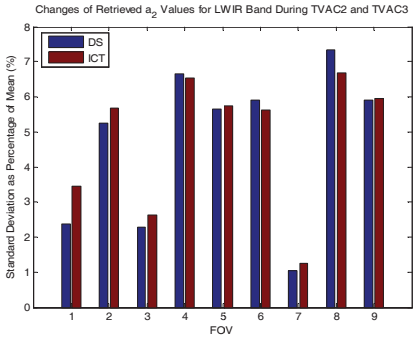

Figure 4. Percentages of changes in the values of a_2 coefficients are in general less than 7% using data collected over a period of several months

5. Conclusion

Our independent analysis of CrIS FM1 TVAC test data supports the performance reported by ITT that this instrument offers excellent radiometric calibration accuracy. Our analysis also helped us identify critical areas that need to be carefully monitored during on-orbit Cal/Val.

Reference

[1] Ronald J. Glumb, David C. Jordan, and Peter Mantica, *Development of the Crosstrack Infrared Sounder (CrIS) Sensor Design,* Infrared Spaceborne Remote Sensing IX, Marija Strojnik, Bjørn F. Andresen, Editors, Proceedings of SPIE Vol. 4486 (2002)

[2] David L. Glackin, John D. Cunningham, Captain Craig S. Nelson, *Earth remote sensing with NPOESS:instruments and environmental data products*, Sensors, Systems, and Next-Generation Satellites VII, edited by Roland Meynart,, Steven P. Neeck, Haruhisa Shimoda, Joan B. Lurie, Michelle L. Aten, Proceedings of SPIE, Vol. 5234, 2004.

[3] Stephen A. Mango; Robert E. Murphy; Hassan Ouaidrari; W. Paul Menzel, *NPOESS Preparatory Project (NPP) instrument characterization and calibration, and products validation: an integrated strategy in preparation for NPOESS new generation of environmental satellites*, SPIE Proceedings, Vol. 4891, Optical Remote Sensing of the Atmosphere and Clouds III, Hung-Lung Huang; Daren Lu; Yasuhiro Sasano, Eds., pp.22-35, April 2003.

[4] Anne Kleinert, *Correction of detector nonlinearity for the balloonborne Michelson Interferometer for Passive Atmospheric Sounding*, APPLIED OPTICS, Vol. 45, No. 3, 20 January 2006, pp.425-431.

[5] R. O. Knuteson, H. E. Revercomb, F. A. Best, N. C. Ciganovich, R. G. Dedecker, T. P. Dirkx, S. C. Ellington, W. F. Feltz, R. K. Garcia, H. B. Howell, W. L. Smith, J. F. Short, and D. C. Tobin, *Atmospheric Emitted Radiance Interferometer (AERI). II. Instrument performance*, J. Atmos. Ocean. Technol. 21, 1777–1789, Dec. 2004.